

Is lobular endocervical glandular hyperplasia a cancerous precursor of minimal deviation adenocarcinoma? : A comparative molecular-genetic and immunohistochemical study

Shigeto Kawauchi¹, M.D., Tomoko Kusuda¹, M.D., Xu-Ping Liu¹, M.D., Yutaka Suehiro², M.D., Tsunehisa Kaku³, M.D., Yoshiki Mikami⁴, M.D., Morishige Takeshita⁵, M.D., Motonao Nakao¹, Ph.D., Yasuyo Chochi¹, M.D., and Kohsuke Sasaki¹, M.D.

From the Departments of Pathology¹ and Clinical Laboratories², Yamaguchi University Graduate School of Medicine, Yamaguchi; the Department of Health Sciences³, Kyushu University Graduate School of Medicine, Fukuoka; the Department of Surgical Pathology⁴, Kyoto University Hospital, Kyoto; and the Department of Pathology⁵, Fukuoka University School of Medicine, Fukuoka, Japan.

Correspondence and reprint request to:

Shigeto Kawauchi, MD, PhD

Department of Pathology, Yamaguchi University Graduate School of Medicine,

1-1-1 Minamikogushi, Ube, Yamaguchi 755-8505, Japan

Phone: +81 (836) 22-2222, Fax: +81 (836) 22-2223,

e-mail: shig@yamaguchi-u.ac.jp

Abstract

Although lobular endocervical glandular hyperplasia (LEGH) was originally described as a distinct hyperplastic glandular lesion of the uterine cervix, recent studies have raised a question that LEGH may be a cancerous precursor of minimal deviation adenocarcinoma (MDA) and other mucinous adenocarcinomas (MACs) of the uterine cervix. In the present study, we studied LEGH, MDA, and MAC by using molecular-genetic and immunohistochemical methods for chromosomal imbalance, microsatellite instability (MSI), human papillomavirus (HPV) infection, and gastric pyloric-type mucin secretion to clarify their relationship. Comparative genomic hybridization revealed recurrent chromosomal imbalances, *i.e.*, gains of chromosome 3q and a loss of 1p, which were common to MDA and MAC, in three of 14 LEGHs analyzed (21%). LEGHs with chromosomal imbalances showed a degree of cellular atypia in the hyperplastic glandular epithelium. Dual-color fluorescence in situ hybridization confirmed a gain of chromosome 3 fragment in these cervical glandular lesions. HPV in situ hybridization revealed that high risk HPV (types 16 and 18) was positive in over 80% of MACs, but negative in all LEGHs and MDAs examined. MSI was rarely detected in these cervical glandular lesions. Our present study results demonstrated a molecular-genetic link between LEGH and cervical mucinous glandular malignancies including MDA and MAC, and are thought to support the hypothesis that a proportion of LEGHs are cancerous precursors of MDA and/or MAC.

Key words: lobular endocervical glandular hyperplasia; minimal deviation adenocarcinoma; chromosomal imbalance; comparative genomic hybridization; gastric pyloric-type mucin; human papillomavirus; microsatellite instability.

Introduction

Uterine-cervical carcinoma is the second most common malignancy in women worldwide. It has been reported that approximately 80% of them are squamous cell carcinomas while 10-20% are adenocarcinomas [24]. Although recent cervical screening programs have achieved a decrease in the incidence of cervical squamous cell carcinoma in developed countries, the overall incidence of cervical adenocarcinoma has remained the same or even increased [28,36]. This phenomenon is partially due to the difficulty in diagnosing early or well-differentiated cervical glandular malignancies. Minimal-deviation adenocarcinoma (MDA) of the uterine cervix, *i.e.*, adenoma malignum, is defined as an extremely well differentiated variant of cervical adenocarcinoma, including 1-3% of all cervical glandular malignancies [16]. Histopathologically, MDAs, most of which are mucinous adenocarcinomas, are recognized to be malignant by the presence of evident cancerous glands at least focally accompanied by a desmoplastic stromal reaction [3,29,35]. A diagnosis of MDA is sometimes problematic because of its mostly bland-looking tumor cell appearance and lack of evident diagnostic criteria. However, because cervical adenocarcinomas are usually resistant to conventional radiotherapy and chemotherapy, an accurate diagnosis of MDA is important for both pathologists and clinicians.

In 1999, Nucci *et al.* first described lobular endocervical glandular hyperplasia (LEGH) as a distinct hyperplastic glandular lesion of the uterine cervix [22]. It is important to distinguish LEGH from MDA because they share some clinical and histological features, *e.g.*, abundant watery vaginal discharge and cystically dilated endocervical glands [22]. Although LEGH was first described as a hyperplastic glandular lesion of the uterine cervix, some pathologists have noticed that LEGH may show a degree of glandular cellular atypia [21,14]. Furthermore, recent studies

have revealed that most MDAs demonstrate a gastric phenotype as shown by the presence of cancerous glands secreting gastric pyloric-type mucin [9]. Interestingly, LEGHs have also been shown to secrete gastric pyloric-type mucin as well [20]. These observations have made us to consider that a proportion of LEGHs may be a cancerous precursor of MDA.

There are some molecular-genetic studies of cervical adenocarcinomas [7,30,34], however, their cancerous precursors have rarely been addressed in these studies. Furthermore, molecular-genetic aberrations of LEGH and MDA, and their possible genetic correlation have yet to be investigated well. In the present study, LEGH, MDA and other types of cervical mucinous adenocarcinoma (MAC) were analyzed using some molecular-genetic and immunohistochemical methods in an attempt to clarify their relationship. The aim of the present study was to gain an insight into LEGH as a possible cancerous precursor based on not only histological and immunohistochemical factors but also molecular-genetic aspects.

Materials and Methods

Materials

The present study followed the ethical guidelines of the Institutional Review Board of the Yamaguchi University School of Medicine. 15 LEGHs, 16 MDAs and 15 MACs were retrieved from the department of surgical pathology files of the National Kyushu Medical Center, Yamaguchi University Hospital, and other affiliated hospitals. LEGH was diagnosed by the presence of characteristic lobular architecture composed of small to moderate-sized endocervical glands often surrounding cystically dilated glands (Figures 1A and 1B), however exhibiting neither sufficient cellular atypia for malignancy nor evidence of stromal invasion (Figures 1C and 1D) according to the first description by Nucci, *et al.* [22]. MDA was diagnosed as an extremely well differentiated variant of cervical mucinous adenocarcinoma at least focally exhibiting evident cellular atypia for malignancy and figures of stromal invasion [3,16]. MACs were classified into endocervical and intestinal types according to the WHO classification, 2002 [29]. For each cervical glandular lesion, the most representative one or two paraffin-embedded tissue blocks were selected.

Immunohistochemistry and in situ hybridization

Immunohistochemical staining for gastric pyloric-type mucin was performed using a HISTOFINE SAB-PO (M) Immunohistochemical Staining Kit (Nichirei, Tokyo, Japan) according to the manufacturer's description. A mouse monoclonal antibody against gastric pyloric-type mucin, clone HIK1083, (diluted at 1:50, Kanto-Kagaku, Tokyo, Japan) was used as primary antibody [20,21]. In the evaluation, gastric pyloric-type mucin was considered positive when >10% of glandular or cancerous cells were stained positively in the cytoplasm.

In situ hybridization for high-risk HPV was done using a commercially available biotinylated

HPV DNA probe mixture for HPV types 16 and 18 (Y1412, Dako, Tokyo, Japan) according to the manufacturer's instruction. Briefly, a 4- μ m-thick formalin-fixed, paraffin-embedded sample tissue section was deparaffinized in xylene and pretreated by microwave irradiation and pepsin digestion. Approximate 60 μ l of the HPV DNA probe mixture was dropped on a pretreated sample tissue section, denatured at 95°C for 5 min, and hybridized at 37°C for 16 hr using a programmable temperature control system (PC-816, ASTEC, Fukuoka, Japan). The slide was washed, incubated with streptavidin-alkaline phosphatase solution (Dako), and then visualized with nitroblue tetrazolium/bromo-4-chloro-3-indolylphosphatase (NBT/BCIP). For the evaluation, high-risk HPV was considered positive when >10% of glandular or cancerous cell nuclei were stained positively.

DNA extraction

10- μ m-thick formalin-fixed, paraffin-embedded sample tissue sections were deparaffinized in xylene, rehydrated in a graded series of ethanol solutions, and stained with methylgreen (Cosmo-Bio, Tokyo, Japan). Atypical glandular lesions of LEGH, as well as the cancerous lesions of MDA and MAC, were microdissected using a 28-gauge needle under a microscopic observation. When glandular lesions mimicking LEGH were observed in MDA or MAC sections, sample DNA was collected solely from the evidently cancerous lesions. Sample genomic DNA was extracted from the microdissected tissues according to a previously described method [11]. Genomic DNA was also extracted from normal endocervical glands of the same sample tissue sections and served as references in the analysis of microsatellite instability (MSI).

CGH

Whole genome amplification of sample DNA and subsequent comparative genomic hybridization (CGH) was according to a previously described method [8,12]. DNA that was

extracted from the peripheral blood lymphocytes of a healthy female donor was used as reference. Sample and reference DNAs were separately amplified by two-phase degenerate oligonucleotide-primed PCR and labeled with spectrumgreen-dUTP (Vysis, Downers Grove, IL) and spectrumorange-dUTP (Vysis) by a standard nick-translation reaction, respectively. Equal amounts of fluorescence-labeled DNAs were dissolved together with Cot-1 DNA (Life Technologies, Rockville, MD) in a CGH hybridization buffer (Vysis). After denaturation, the fluorescence-labeled DNAs were co-hybridized onto a denatured normal metaphase spread slide (Vysis) and incubated at 37°C for 72 hr. The slide was then washed and counterstained with 4,6-diamino-2-phenylindole antifade solution (DAPI-II Counterstain, Vysis). Fluorescence images of the chromosomes were captured and analyzed using the QUIPS XL software program (Vysis). Chromosomal imbalances, *i.e.*, the DNA sequence copy number gain, amplification (high level gain), and the loss were defined as sample-to-reference DNA ratios of >1.2, >1.4, and <0.8, respectively.

Dual-color FISH

Dual-color fluorescence in situ hybridization (FISH) was performed on formalin-fixed, paraffin-embedded tissue sections according to a method described previously [13]. Briefly, 4- μ m-thick formalin-fixed, paraffin-embedded sample tissue sections were deparaffinized and pretreated by pepsin digestion and microwave irradiation techniques. Each 1.0 μ l of chromosome 3 alpha-satellite DNA probe labeled with spectrumorange (CEP3, Vysis) and chromosome 3 whole-paint DNA probe labeled with spectrumgreen (WCP3, Vysis) was dissolved together with a 10 μ l of 1x hybridization buffer (Vysis). The probe mixture was heat-denatured and hybridized onto a heat-denatured sample tissue section. The section was incubated at 37°C for 72 hr, washed in a

series of washing solutions (Vysis), and then mounted with DAPI-II counterstain (Vysis). At least 100 non-overlapping nuclei were observed under a fluorescence microscope and numbers of the fluorescence signals were counted. Percentage of chromosome 3 whole-paint signals for chromosome 3 centromeric signals was calculated on atypical glandular or cancerous lesions of the sample tissue section, and was recorded as a sample chromosome 3 index (sC3I) value. The percentage was also calculated on normal glandular regions of the same sample tissue section, and was recorded as a reference chromosome 3 index (rC3I) value. The chromosome 3 index (C3I) of the sample tissue section was defined as $sC3I/rC3I$.

MSI and methylation-specific PCR for hMLH1 gene promoter

Sample and corresponding reference DNAs were separately amplified by PCR for five microsatellite loci, *i.e.*, D2S123, D5S346, D17S250, BAT25 and BAT26 [1]. The PCR primers were obtained from MapPairs (Research Genetics, Huntsville, AL, USA). 50-100 ng of DNA was dissolved in a 25 μ l of 1x KOD Plus PCR buffer solution (TOYOBO, Toyama, Japan) containing 1.0 μ M primers, 1.5mM MgCl₂, each 0.2 μ M dNTP, and 0.5 unit KOD Plus DNA polymerase (TOYOBO). The PCR conditions were as follows; an initial denaturation at 94°C for 3 min, followed by 37 cycles of each 30 seconds at 94°C, 53-57°C, and 68°C, and a final extension at 68°C for 5 min. The PCR products were separated using a GenePhor Electrophoresis Unit (Amersham Pharmacia, Tokyo, Japan) equipped with a 7.5% polyacrylamide gel containing 5M urea (GeneGel Clean 15/24, Amersham Pharmacia). MSI was estimated according to the National Cancer Institute criteria [1]; high-frequency MSI (MSI-H) when >30% of the microsatellites examined were instable for informative loci, low-frequency MSI (MSI-L) when <30% of microsatellites examined were instable, and microsatellite stable (MSS) when all the microsatellites examined were stable.

The sample DNAs were further forwarded to methylation-specific PCR to examine cytosine hypermethylation of hMLH1 gene promoter CpG islands according to a method described previously [15].

Results

Clinicopathologic findings, immunohistochemistry and in situ hybridization

The age of the patients ranged from 37 to 56 years (mean; 47 years) in LEGH, from 41 to 77 years (mean; 57.5 years) in MDA, and from 42 to 75 years (mean; 58.3 years) in MAC. At the time of initial treatment, the clinical stages according to the International Federation of Gynecology and Obstetrics criteria [7] were as follows; 4 stage IA, 11 stage IB, and 1 stage II tumors in MDAs and 3 stage IA, 10 stage IB, and 2 stage II tumors in MACs. In 3 of 16 MDAs (19%), carcinomas were focally accompanied by LEGH-like hyperplastic glands.

Immunohistochemically, all the 15 LEGHs and 16 MDAs examined were positive for gastric pyloric-type mucin in the cytoplasm of hyperplastic glandular cells (Figure 1E) and adenocarcinoma cells, respectively. Although all the 15 MACs examined were negative for gastric pyloric-type mucin, 2 of the 15 MACs (13%) contained carcinoma cells with positive immunoreactivity for the antigen at least focally. In MDAs with LEGH-like hyperplastic glands, both cancerous and hyperplastic glandular portions were positive for gastric pyloric-type mucin. As for in situ hybridization, all the 15 LEGHs and 16 MDAs examined were negative for high-risk HPV DNA. Two of the 15 MACs (13%) examined were negative for high-risk HPV DNA. The remaining 13 MACs (87%) were positive for high-risk HPV DNA (Figure 1F).

CGH

Informative CGH was possible in 34 (14 LEGHs, 11 MDAs, and 9 MACs) of the 46 DNA samples extracted from formalin-fixed paraffin-embedded tissues (Figure 1G). Aberrant CGH profiles were present in 3 of 14 LEGHs (21%), 10 of 11 MDAs (91%), and 8 of 9 MACs (89%) (Table 1). The average numbers of chromosomal imbalances, *i.e.*, chromosome DNA copy number

gains and losses, per sample were 0.7 in LEGH, 4.2 in MDA, and 3.8 in MAC. In LEGHs, aberrant CGH profiles were detected in DNA samples extracted from the hyperplastic glandular cells with a degree of nuclear atypia, *i.e.*, nuclear elongation, enlargement, and hyperchromasia (Figures 1C and 1D). In LEGHs, the average number of DNA copy number gains was larger than that of the losses (0.42 gain/sample and 0.29 loss/sample). In MDAs and MACs, the average numbers of chromosome DNA copy number gains were smaller than those of the losses (1.5 gain/sample and 2.6 loss/sample, and 1.7 gain/sample and 2.1 loss/sample, respectively). The total number of chromosomal imbalances tended to increase in correlation with the degree of nuclear atypia of the cells analyzed. The frequency of recurrent chromosomal imbalances were; 3q gain (3 of 14 samples analyzed by CGH, 21%) and 1p loss (2 of 14, 13%) in LEGHs (Figure 2A); 3q gain (5 of 11, 45%), 9q gain (3 of 11, 27%), 1p loss (4 of 11, 36%), and 5q loss (3 of 11, 27%) in MDAs (Figure 2B); and 3q gain (4 of 9, 44%), 1p loss (6 of 9, 67%), and 10q loss (5 of 9, 56%) in MACs (Figure 2C). Overall, the 3q gain (12 of 34, 35%) and 1p loss (10 of 34, 29%) were the most common chromosomal imbalances detected in LEGHs, MDAs and MACs.

Dual-color FISH

The dual-color FISH experiments were performed to confirm chromosome 3q gain on the formalin-fixed, paraffin-embedded tissue sections of 2 LEGHs (Figure 1H), 3 MDAs and 2 MACs whose 3q gains were detected in the CGH analysis. sC3I and rC3I values were 2.28 to 2.77 and 1.39 to 1.62, respectively. In all lesions, the sC3I values were constantly larger than the rC3I values on the same sample tissue sections (Table 2). The C3I (= sC3I/rC3I) values were 1.55 to 1.78 in all cervical glandular lesions examined. The result indicated an increase of DNA fragments of chromosome 3 and was compatible with the above CGH finding.

MSI and MSP for hMLH-1 gene promoter

MSI-L was shown in each MDA and MAC (Table 1, A7 and M6). Both carcinomas demonstrated chromosomal imbalances in the CGH analysis. Cytosine methylation of hMLH-1 gene promoter CpG islands was proved by MSP in one case of MAC with MSI-L (Figure 3, M6).

Discussion

Cervical cancers are now recognized as HPV-related tumors [2,37]. The oncoproteins E6 and E7, which are encoded in high-risk HPV types 16, 18 and *et al.*, exploit the ubiquitin-proteasome system to degrade and inactivate the p53 and RB tumor suppressor gene products, leading to cervical carcinogenesis. Previous studies also revealed a high incidence of high-risk HPV in adenocarcinomas in situ and invasive adenocarcinomas of the uterine cervix [2,37]. Interestingly, recent studies have reported a rather low incidence of HPV in both LEGHs and MDAs [21,32], which is comparable to our present study result of HPV in situ hybridization. These findings seemed to suggest a close relationship between LEGH and MDA, as well as possibly different carcinogenic pathways between MDA and MAC. In an attempt to answer these questions, in the present study, LEGH, MDA, and MAC were analyzed using some molecular-genetic methods.

CGH was initially introduced as a tool to screen chromosomal imbalances in tumors [10], but the method has rarely been applied to a cell lineage analysis. A cell lineage analysis is based on genetic markers unique to the cell lineage to be analyzed [31]. In a classical banding chromosome analysis, chromosomal aberrations, *e.g.*, position of breakpoints and presence of marker chromosomes, have been used as lineage markers. Thus, specific chromosomal aberrations detected by CGH, *e.g.*, position of breakpoints and pattern of nonrandom chromosomal imbalances, are thought to provide markers to analyze sequential progression of a cancerous precursor to cancer [31].

In the present CGH study, three of 14 LEGHs (21%) showed recurrent chromosomal imbalances that were common to MDA, *i.e.*, gain of chromosome 3q and a loss of 1p (Table 1 and Figures 2A-C). Because the present DNA samples of LEGH were extracted from somewhat atypical glandular epithelium by using microdissection technique, the CGH results imply that LEGH with

cellular atypia possesses chromosomal imbalances related to MDA. Furthermore, in the present study, some MDAs were concomitant with hyperplastic glandular lesions mimicking LEGH as described previously [14,21]. In such MDA with LEGH-like region, the LEGH-like hyperplastic glands demonstrated gastric pyloric-type mucin secretion as well as the cancerous lesions. These evidences are consistent with the hypothesis that some LEGHs are cancerous precursors of MDA.

Among recurrent chromosomal imbalances detected in the present CGH analysis, 3q gain was the aberration detected most frequently. Recent molecular-genetic studies have reported that 3q gain occurs frequently in both precancerous and cancerous lesions of the uterine cervix, including cervical intraepithelial neoplasia, squamous cell carcinomas, and adenocarcinomas [6,7,30,34]. Furthermore, 3q gain is associated with the progression from high-grade intraepithelial neoplasia to invasive carcinoma [6]. Some investigators thus consider 3q gain to be one of the most important genetic events that are linked with the acquisition of malignant phenotype in cervical carcinogenesis. A number of genes located at chromosome 3q, *e.g.*, PIK3CA [19], eIF-5A2 [4] and CCNL1 [27], have been implicated as possible candidate oncogenes that are associated with gain or amplification of 3q. Further studies, *e.g.*, array-based CGH, will be necessary to validate the consideration.

FISH analysis was suitable to correlate chromosomal imbalances with histological findings of tissue sections. Because atypical glandular or cancerous lesions from which sample DNAs were extracted were usually sporadic on the sample tissue sections, dual-color FISH with chromosome 3-pericentromeric and chromosome 3 whole-paint probes was used to confirm the chromosome 3q gain that was detected in the present CGH analysis [26,33]. Furthermore, because nuclear truncation might result in a reduced number of FISH signals on a sample tissue section, sC3I, rC3I

and C3I were devised and applied to estimate the chromosome 3 imbalances. In the current FISH analysis, the sC3I values were constantly larger than the rC3I values in all the cervical glandular lesions examined. Therefore, the FISH result indicated an increase of DNA fragments of chromosome 3 and was compatible with the CGH result, *i.e.*, 3q gain.

In general, genetic instability is considered to play a key role in the progression of multistep carcinogenesis by accumulating various genetic aberrations [5]. From studies of colorectal and other cancers, cancers with genetic instability have been classified into two categories, *i.e.*, the chromosomal instability (CIN) phenotype and the microsatellite instability (MSI) phenotype [17,18]. The majority of cancers belongs to the CIN phenotype and is characterized by abnormal chromosome number. In a fraction of cancers, mismatch repair deficiency leads to the MSI phenotype with genetic aberrations at the nucleotide sequence level. MSI is caused by deficient DNA mismatch repair. A loss of hMLH1 protein, one of the major DNA mismatch repair gene products, is thought to be a potent trigger of MSI [25].

Our present study revealed that most MDAs and MACs examined had chromosomal imbalances, suggesting CIN phenotype to be the major category to which these cervical adenocarcinomas belong. Although MSI-L was detected in each MDA and MAC among the cervical glandular lesions examined in the present study, these two tumors with MSI-L also carried a moderate degree of chromosomal imbalances (Table 1). Therefore, CIN phenotype with secondary MSI is preferred to pure MSI phenotype concerning these cervical adenocarcinomas with MSI-L. Furthermore, cytosine hypermethylation of hMLH1 gene promoter CpG islands, one of the causes of hMLH1 gene silencing, was thought to be a rare event in the present study, which supports our consideration described above.

In conclusion, some LEGHs that were examined in the present study shared nonrandom chromosomal imbalances with MDAs and MACs. In addition to the histological findings, immunohistochemistry for gastric pyloric-type mucin, and the HPV in situ hybridization result, the present molecular-genetic findings support that some LEGHs are cancerous precursors of MDA and/or MAC. The present study results are likely to support a clinical treatment of LEGH as a precursor of cervical adenocarcinoma.

Acknowledgments

The authors appreciate Prof. Robert H. Young, Massachusetts General Hospital, for his advice regarding our diagnosis of some LEGH cases. We also thank Dr. Kenichi Nishiyama, the National Kyushu Cancer Center, for providing us with some tumor samples. The present study was supported in part by a grant-in-aid from the New Energy and Industrial Technology Development Organization (Grant no. 03A47023d) and a grant-in-aid from the Japan Society for the Promotion of Science (Grant no. 18590330).

References

1. Boland CR, Thibodeau SN, Hamilton SR, et al. A National Cancer Institute workshop on microsatellite instability for cancer detection and familial predisposition: development of international criteria for the determination of microsatellite instability in colorectal cancer. *Cancer Res.* 1998; 58: 5248-5257.
2. Ferguson AW, Svoboda-Newman SM, Frank TS. Analysis of human papillomavirus infection and molecular alterations in adenocarcinoma of the cervix. *Mod Pathol.* 1998; 11: 11-18.
3. Gilks CB, Young RH, Aguirre P, DeLellis RA, Scully RE. Adenoma malignum (minimal deviation adenocarcinoma) of the uterine cervix: a clinicopathological and immunohistochemical analysis of 26 cases. *Am J Surg Pathol.* 1989; 13: 717-729.
4. Guan XY, Sham JS, Tang TC, Fang Y, Huo KK, Yang JM. Isolation of a novel candidate oncogene within a frequently amplified region at 3q26 in ovarian cancer. *Cancer Res.* 2001; 61: 3806-3809.
5. Hanahan D, Weinberg RA. The hallmarks of cancer. *Cell.* 2000; 100: 57-70.
6. Heselmeyer K, Schrock E, du Manoir SD, et al. Gain of chromosome 3q defines the transition from severe dysplasia to invasive carcinoma of the uterine cervix. *Proc Natl Acad Sci USA.* 1996; 93: 479-484.
7. Hirai Y, Utsugi K, Takeshima N, et al. Putative gene loci associated with carcinogenesis and metastasis of endocervical adenocarcinomas of uterus determined by conventional and array-based CGH. *Am J Obstet Gynecol.* 2004; 191: 1173-1182.
8. Hirose Y, Aldape K, Takahashi M, Berger MS, Feuerstein BG. Tissue microdissection and degenerate oligonucleotide primed-polymerase chain reaction (DOP-PCR) is an effective

- method to analyze genetic aberrations in invasive tumors. *J Mol Diagn.* 2001; 3: 62-67.
9. Ishii K, Hosaka N, Toki T, et al. A new view of the so-called adenoma malignum of the uterine cervix. *Virchows Arch.* 1998; 432: 315-322.
 10. Kallioniemi A, Kallioniemi OP, Sudar D, et al. Comparative genomic hybridization for molecular cytogenetic analysis of solid tumors. *Science.* 1992; 258: 818-821.
 11. Kawauchi S, Liu XP, Kawasaki K, et al. Significance of β -catenin and pRB pathway components in malignant ovarian germ cell tumours: INK4A promoter CpG island methylation is associated with cell proliferation. *J Pathol.* 2004; 204: 268-276.
 12. Kawauchi S, Okuda S, Morioka H, et al. Large cell neuroendocrine carcinoma of the uterine cervix with cytogenetic analysis by comparative genomic hybridization: a case study. *Hum Pathol.* 2005; 36: 1096-1100.
 13. Kitayama Y, Igarashi H, Sugimura H. Initial intermittent microwave irradiation for fluorescence in situ hybridization analysis in paraffin-embedded tissue sections of gastrointestinal neoplasia. *Lab Invest.* 2000; 80: 779-781.
 14. Kondo T, Hashi A, Murata S, et al. Endocervical adenocarcinomas associated with lobular endocervical glandular hyperplasia: a report of four cases with histochemical and immunohistochemical analyses. *Mod Pathol.* 2005; 18: 1199-1210.
 15. Kondo Y, Shen L, Issa JP. Critical role of histone methylation in tumor suppressor gene silencing in colorectal cancer. *Mol Cell Biol.* 2003; 23: 206-215.
 16. Kurman RJ, Norris HJ, Wilkinson E. Tumors of the Cervix. In: Rosai J, Sobin LH, eds. *Atlas of tumor pathology, tumors of the cervix, vagina and vulva, 3rd Series.* Washington DC: AFIP, 1992: 91-93.

17. Lengauer C, Kinzler KW, Vogelstein B. Genetic instabilities in colorectal cancers. *Nature*. 1997; 386: 623-627.
18. Lengauer C, Kinzler KW, Vogelstein B. Genetic instabilities in human cancers. *Nature*. 1998; 396: 643-649.
19. Ma YY, Wei SJ, Lin YC, et al. PIK3CA as an oncogene in cervical cancer. *Oncogene*. 2000; 19: 2739-2744.
20. Mikami Y, Hata S, Melamed J, Fujiwara K, Manabe T. Lobular endocervical glandular hyperplasia is a metaplastic process with a pyloric gland phenotype. *Histopathology*. 2001; 39: 364-372.
21. Mikami Y, Kiyokawa T, Hata S, et al. Gastrointestinal immunophenotype in adenocarcinomas of the uterine cervix and related glandular lesions: a possible link between lobular endocervical glandular hyperplasia/pyloric gland metaplasia and 'adenoma malignum'. *Mod Pathol*. 2004; 17: 962-972.
22. Nucci MR, Clement PB, Young RH. Lobular endocervical glandular hyperplasia, not otherwise specified: a clinicopathologic analysis of thirteen cases of a distinctive pseudoneoplastic lesion and comparison with fourteen cases of adenoma malignum. *Am J Surg Pathol*. 1999; 23: 886-891.
23. Peng DF, Sugihara H, Mukaisho K, Ling ZQ, Hattori T. Genetic lineage of poorly differentiated gastric carcinoma with a tubular component analyzed by comparative genomic hybridization. *J Pathol*. 2004; 203: 884-895.
24. Pisani P, Bray F, Parkin DM. Estimates of the world-wide prevalence of cancer for 25 sites in the adult population. *Int J Cancer*. 2002; 97: 72-81.

25. Prolla TA, Pang Q, Alani E, Kolodoner RD, Liskay RM. MLH1, PMS1, and MSH2 interactions during the initiation of mismatch repair in yeast. *Science*. 1994; 265: 1091-1093.
26. Qian J, Bostwick DG, Takahashi S, et al. Comparison of fluorescence in situ hybridization analysis of isolated nuclei and routine histological sections from paraffin-embedded prostatic adenocarcinoma specimens. *Am J Pathol*. 1996; 149: 1193-1199.
27. Redon R, Hussenet T, Bour G, et al. Amplicon mapping and transcriptional analysis pinpoint cyclin L as a candidate oncogene in head and neck cancer. *Cancer Res*. 2002; 62: 6211-6217.
28. Smith HO, Tiffany MF, Qualls CR, Kay CR. The rising incidence of adenocarcinoma relative to squamous cell carcinoma of the uterine cervix in the United States: a 24-year population based study. *Gynecol Oncol*. 2000; 78: 97-105.
29. Wells M, Nesland JM, Oster AG, et al. Tumours of the uterine cervix. In: Tavassoli FA, Devilee P, eds. *World health organization classification of tumours: pathology and genetics of tumours of the breast and female genital organs*. Lyon: IARC Press, 2003: 272-277.
30. Wilting SM, Snijders PJ, Meijer GA, et al. Increased gene copy numbers at chromosome 20q are frequent in both squamous cell carcinomas and adenocarcinomas of the cervix. *J Pathol*. 2006; 209: 220-230.
31. Wolman SR. Karyotypic progression of human tumors. *Cancer Metast Rev*. 1983; 2: 257-293.
32. Xu JY, Hashi A, Kondo T, et al. Absence of human papillomavirus infection in minimal deviation adenocarcinoma and lobular endocervical glandular hyperplasia. *Int J Gynecol Pathol*. 2005; 24: 296-302.
33. Yang P, Hirose T, Hasegawa T, Hizawa K, Sano T. Dual-color fluorescence in situ hybridization analysis of synovial sarcoma. *J Pathol*. 1998; 184: 7-13.

34. Yang YC, Shyong WY, Chang MS, et al. Frequent gain of copy number on the long arm of chromosome 3 in human cervical adenocarcinoma. *Cancer Genet Cytogenet.* 2001; 131: 48-53.
35. Young RH, Clement PB. Endocervical adenocarcinoma and its variants: their morphology and differential diagnosis. *Histopathology.* 2002; 41: 185-207.
36. Zappa M, Visioli CB, Ciatto S, Iossa A, Paci E, Sasieni P. Lower protection of cytological screening for adenocarcinomas and shorter protection for younger women: the results of a case-control study in Florence. *Br J Cancer.* 2004; 90: 1784-1786.
37. Zielinski GD, Snijders PJ, Rozendaal L, et al. The presence of high-risk HPV combined with specific p53 and p16INK4a expression patterns points to high-risk HPV as the main causative agent for adenocarcinoma in situ and adenocarcinoma of the cervix. *J Pathol.* 2003; 201: 535-543.

Figure Legends

Figure 1. Lobular endocervical glandular hyperplasia (LEGH) of the uterine cervix (case L1). (A) Grossly, cystically dilated cervical glands are located in the uterine cervix. (B) Microscopically, lobules that are composed of aggregated endocervical glands are observed around cystically dilated endocervical glands. (C) Focally, endocervical glands are lined by atypical glandular epithelium with tufting of the glandular cells and pseudostratification of the nuclei. (D) Endocervical glands that are focally accompanied by glandular cells with enlarged atypical nuclei. (E) Immunohistochemical staining for gastric pyloric-type mucin. The hyperplastic cervical glandular cells are positive for gastric pyloric-type mucin in the cytoplasm. (F) In situ hybridization for high-risk human papillomavirus (HPV) DNA types 16 and 18. The hyperplastic cervical glandular cells of LEGH are negative for high-risk HPV DNA (left, case L1). Adenocarcinoma cells are positive for high-risk HPV DNA (right, case M2). (G) Representative image of hybridized normal metaphase chromosomes in comparative genomic hybridization for genomic DNA extracted from the formalin-fixed, paraffin-embedded LEGH tissue. (H) Dual-color fluorescence in situ hybridization on a section of the formalin-fixed, paraffin-embedded LEGH tissue. Chromosome 3 whole-paint signals (green) and chromosome 3-pericentromeric signals (red) are observed.

Figure 2. The rate of chromosomal gains and losses observed in non-acrocentric chromosomal arms of 14 lobular endocervical glandular hyperplasias (A), 11 minimal deviation adenocarcinomas (B) and 9 cervical mucinous adenocarcinomas (C). Each bar represents the percentage of gain (upper) and loss (lower) of a chromosomal arm.

Figure 3. Methylation-specific PCR for cytosine hypermethylation of hMLH1 gene promoter CpG

islands. Primer sets used for amplification are designated as methylated (m) and unmethylated (u). Small arrow indicates hMLH1 gene promoter methylation (M6). M1 to M6, sample number: S, size marker: MSP, methylation-specific PCR.

Table 1. Summary of CGH, MSI, in situ hybridization and immunohistochemistry results

Histology	Sample	GM-IHC	HPV-ISH	MSI	CGH
LEGH	L1	p	n	s	loss: 1p32-pter gain: 2q23-32, 3q21-28, 20q
	L2	p	n	s	loss: 1p31-pter, 11q23-24 gain: 3q22-28,
	L3	p	n	s	loss: 19q31-qter gain: 3q22-25, 5q15-22
	L4	p	n	s	loss: n gain: n
	L5	p	n	s	loss: n gain: n
	L6	p	n	s	loss: n gain: n
	L7	p	n	s	loss: n gain: n
	L8	p	n	s	loss: n gain: n
	L9	p	n	s	loss: n gain: n
	L10	p	n	s	loss: n gain: n
	L11	p	n	s	loss: n gain: n
	L12	p	n	s	loss: n gain: n
	L13	p	n	s	loss: n gain: n
	L14	p	n	s	loss: n gain: n
MDA	A1	p	n	s	loss: 1p32-pter, 4p15.1-pter, 9q31-qter, 16q21-qter, 19p gain: 3q13-qter, 5q31-qter, 12q21-23
	A2	p	n	s	loss: 9q33-qter, 22q gain: 2q23-q24, 3q12-q28, 5q12-q23, 6q25-cent
	A3	p	n	s	loss: 10q25-qter, 16p12, 16q22-qter gain: 3q22-27
	A4	p	n	s	loss: 3p14-pter, 9q21-33, 10q22-qter gain: 3q21-cen
	A5	p	n	s	loss: 1p32-36, 8p12-pter, 9q21-qter, Xq25-27 gain: 3q21-cen, 5q31-qter
	A6	p	n	s	loss: 3p13-25, 4p15.1-pter, 8p21-23, 11p14-pter, 12p11.2-pter gain: 3q23-24, 9q21-cen
	A7	p	n	l	loss: 8q31-qter, 11q22-23, Xq25-27 gain: 9q22-cen
	A8	p	n	s	loss: 1p33-pter, 8p12-pter gain: 12q21-22
	A9	p	n	s	loss: 1p32-pter gain: 20q12-qter
	A10	p	n	s	loss: 22q gain: 11q23-qter
	A11	p	n	s	loss: n gain: n
MAC	M1	n	p	s	loss: 20q12-qter gain: 3q22-27
	M2	n	p	s	loss: 20q gain: 3q24-qter, 11p14-cen
	M3	n	p	s	loss: 10q22-qter gain: 3q26-qter, 11p14-cen
	M4	n	p	s	loss: 1p32-pter, 2q12-22, 11q13-qter, Xp11.2-pter gain: 4q22-26, 5q14-21, 17q22-24
	M5	n	p	s	loss: 1p31-pter, 8p21-pter, 10q22-qter, 11p12-pter gain: 2q22-24, 4q13-32, 6q21-23
	M6	n	p	l	loss: 1p32-pter, 16q21-qter, 20q12-qter gain: 2p21-16, 5q14-21
	M7	n	n	s	loss: 1p31-pter, 2p22-pter, 22q gain: 13q21-22
	M8	p	p	s	loss: 2q12-21, 3q14-21, 10q25-26 gain: 11q23.1
	M9	n	p	s	loss: n gain: n

LEGH: lobular endocervical glandular hyperplasia (L1-L14) p: positive
MDA: minimal deviation adenocarcinoma (A1-A11) n: negative
MAC: mucinous adenocarcinoma of the uterine cervix (M1-M9) s: microsatellite stable
GM-IHC: immunohistochemistry for gastric pyloric-type mucin l: microsatellite instability low
HPV-ISH: in situ hybridization for human papillomavirus types 16 and 18
MSI: microsatellite instability M1 to M5 are mucinous adenocarcinoma, endocervical type.
CGH: comparative genomic hybridization M6 to M9 are mucinous adenocarcinoma, intestinal type.

Table 2. Dual-color FISH and chromosome 3 index

sample	sC3I	rC3I	C3I
L1	2.44	1.51	1.62
L2	2.51	1.62	1.55
A1	2.53	1.61	1.57
A2	2.64	1.58	1.67
A3	2.28	1.39	1.64
M1	2.77	1.56	1.78
M2	2.48	1.49	1.66

sC3I: sample chromosome 3 index

rC3I: reference chromosome 3 index

C3I: chromosome 3 index

L1 and L2: lobular endocervical glandular hyperplasia

A1 to A3: minimal deviation adenocarcinoma

M1 and M2: mucinous adenocarcinoma of the cervix

Figure 1.

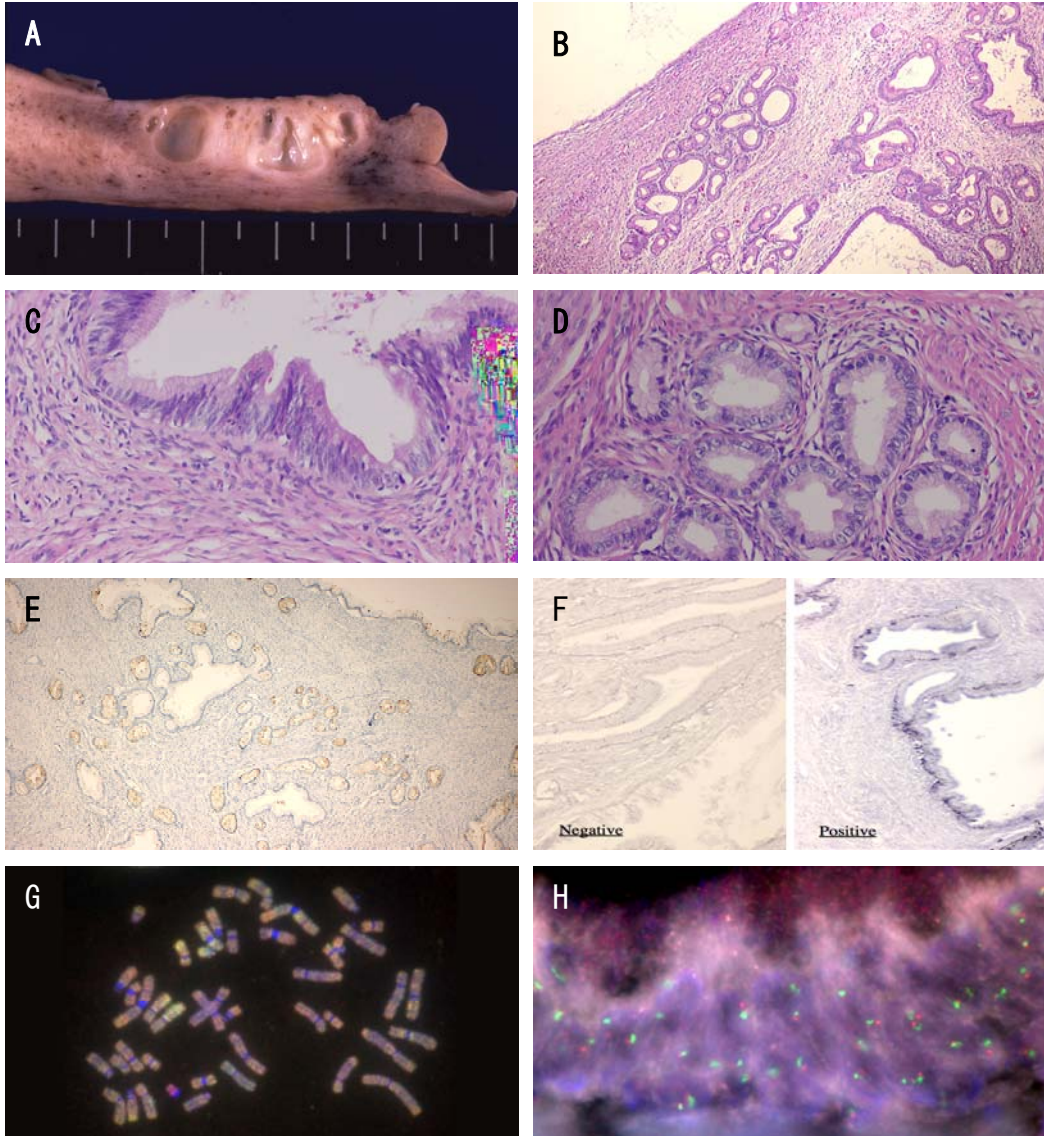


Figure 2A.

Lobular endocervical glandular hyperplasia

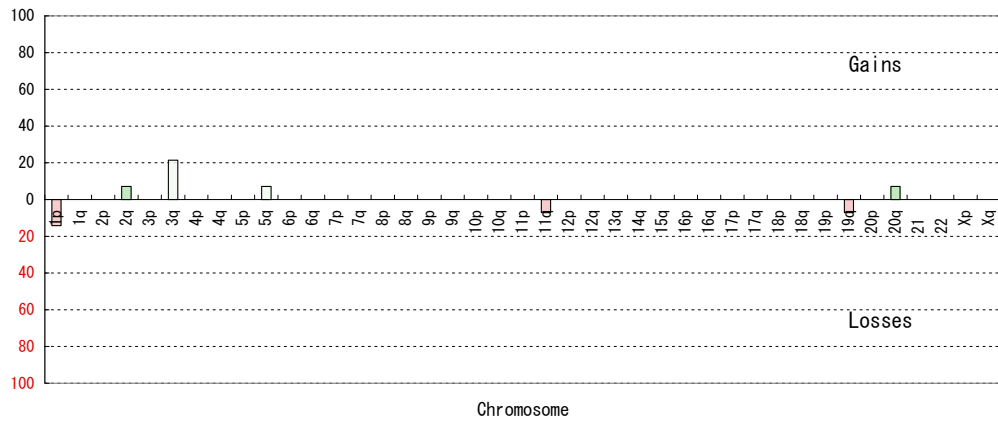


Figure 2B.

Minimal deviation adenocarcinoma

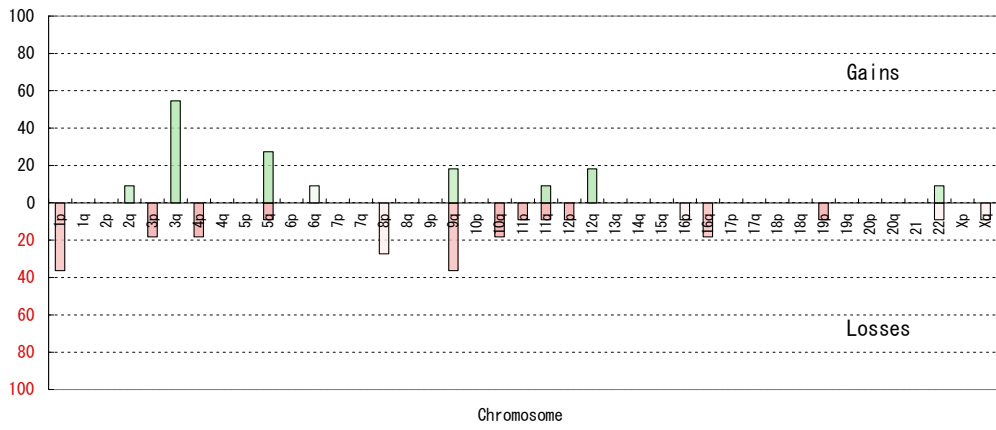


Figure 20.

Mucinous adenocarcinoma

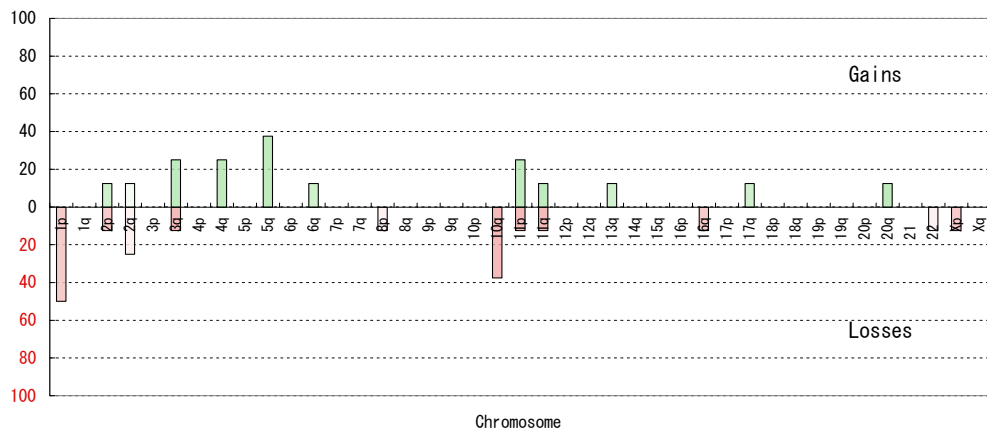


Figure 3.

